evoked consistent ocular following and, as Fig. 2A shows for one animal, once again the response varied inversely with the viewing distance. The maximum compensatory eye speeds achieved within 100 ms of the onset of stimulus motion are plotted in Fig. 2B, from which it is evident that OFR responses were a linear function of the inverse of the viewing distance. Similar data were obtained from all four animals. When the data from each animal were expressed as a percentage of that same animal's highest mean response and plotted against the inverse of the viewing distance, there was surprisingly little variation: the range of slopes was only 14% to 16% per diopter (mean, 15% per diopter), and the range of intercepts was 22% to 34% (mean, 28%).

That the OFR shares the TVOR's dependence on proximity leads us to suggest that the two reflexes share a pathway whose efficacy is modulated by absolute distance cues (*9*). Further, we suggest that these two systems are synergistic, functioning to compensate selectively for translational disturbances of the observer (*10*). In our proposed scheme (see Fig. 3), the TVOR and OFR share two gain elements: a variable one (k_1/d, where k_1 is a constant and d is the target distance), which gives the dependence on proximity, and a fixed one (k_2), which accounts for the offset in our data. The variable gain element allows the TVOR to receive inputs encoded in Cartesian coordinates [translational velocity of the head ($\dot{H}_T$)] and to respond with outputs coded in polar coordinates [rotational velocity of the eyes ($\dot{E}_R$)]. That the visual contribution enters the system upstream of the variable gain element might seem less than optimal since negative feedback systems such as this function best when their gain is fixed at some maximum limited only by stability considerations. However, we suggest that the variable element helps to offset velocity saturation, which is known to be present in the OFR (*2*) and has been incorporated into Fig. 3. Retinal slip speeds experienced by the moving observer will tend to vary inversely with viewing distance; hence ocular following will tend to show increasing saturation with near viewing, an effect that the gain element, k_1/d, will counteract. Thus, the observed dependence on proximity meets the geometric needs of the TVOR and offsets the intrinsic limitations of the OFR.

REFERENCES AND NOTES

1. The compensatory eye rotation, θ, required to keep the eyes aligned on an object at distance, d, when the observer is moved sideways in a straight line ("lateral translation" along the interaural axis) over a distance, M, is arctan (M/d). Taking derivatives, the velocity of the compensatory eye rotation, θ, is given by the expression:

$$\left[\frac{1}{1+\left(\frac{M}{d}\right)^2}\right]\left(\frac{\dot{M}}{d}\right)$$

In our experiments and most comparable everyday situations, the time scale of interest is brief and $d >> M$, so that the first term approaches 1, hence the required compensatory eye movement effectively becomes $\dot{M}/d$.

2. F. A. Miles, K. Kawano, L. M. Optican, *J. Neurophysiol.* **56**, 1321 (1986); K. Kawano and F. A. Miles, *ibid.*, p. 1355.
3. The otolith organs are also influenced by changes in orientation with respect to the earth's gravity [C. Fernandez, J. M. Goldberg, W. K. Abend, *J. Neurophysiol.* **35**, 978 (1972); C. Fernandez and J. M. Goldberg, *ibid.* **39**, 970 (1976)]. This can give rise to ocular counter-rolling, an otolith-ocular reflex that acts to maintain the orientation of the eyes. We shall not be concerned with this reflex here, which is very weak in monkeys [H. Krejcova, S. Highstein, B. Cohen, *Acta Oto-laryngol.* **72**, 165 (1971)].
4. L. B. W. Jongkees and A. J. Phillipszoon, *Acta Physiol. Pharmacol. Neerl.* **10**, 239 (1962); J. I. Niven, W. C. Hixson, M. J. Correia, *Acta Otolaryngol.* **62**, 429 (1966); A. Buizza, A. Leger, J. Droulez, A. Berthoz, R. Schmid, *Exp. Brain Res.* **39**, 167 (1980).
5. R. W. Baloh, K. Beykirch, V. Honrubia, R. D. Yee, *J. Neurophysiol.* **60**, 2000 (1988).
6. G. D. Paige, D. L. Tomko, D. B. Gordon, *Invest. Ophthalmol. Visual Sci. (Suppl.)* **29**, 342 (1988).
7. Animals had been previously anesthetized with sodium pentobarbital to implant devices for the recording of eye movements; sterile procedures were used (*2*). Animals were trained to fixate target lights by previously described methods (*2*).
8. Our previous studies had shown that ocular following responses are transiently augmented by a prior saccade across a textured scene (*2*), and we made use of this in the present study by having the animal make a 10-degree rightward saccade into the center of the pattern 30 ms before the stimulus motion began. This was achieved by reinforcing the animals for transferring fixation between appropriately positioned target spots projected onto the scene.
9. Additional experiments indicated that the linear dependence of both reflexes on the inverse of the viewing distance was preserved over a range of stimulus motion parameters: sled jerk amplitude was varied from 305 to 940 cm/s^2 per second, and the velocity of the visual scene was varied from 10 to 160 degrees/s. Further data from three of the monkeys indicated that the TVOR responses could be increased by selectively increasing either vergence (by means of base-out prisms with the most distant target) or accommodation (by means of base-in prisms with the nearest target) and these increases in response were similar in the two cases. These findings indicate that the TVOR uses some internal measure of both the vergence and the accommodative states to modulate its gain in accordance with the viewing distance.
10. Others have suggested this on theoretical grounds: K. Nakayama, *Vision Res.* **25**, 625 (1985); J. J. Koenderink, *ibid.* **26**, 161 (1986).

1 June 1989; accepted 10 August 1989

Sequence-Specific Isotope Effects on the Cleavage of DNA by Bleomycin

JOHN W. KOZARICH,* LEROY WORTH, JR., BRUCE L. FRANK, DONNA F. CHRISTNER, DANA E. VANDERWALL, JOANNE STUBBE*

Bleomycin is a metal- and oxygen-dependent DNA cleaver. The chemistry of DNA damage has been proposed to involve rate-limiting abstraction of the 4′-hydrogen. A DNA fragment has been prepared that contains [4′-^{2}H]thymidine residues of high isotopic content. Primary kinetic isotope effects have been directly observed at individual thymidine residues with DNA sequencing technology.

THE ELUCIDATION OF THE MECHANISMS of DNA cleavage by bleomycin (BLM) (*1*), the neocarzinostatin cofactor (*2*), calicheamicin (*3*), esperamicin (*4*), and related compounds (*5*) has been extensively investigated. High sensitivity and precision are required to evaluate the mechanistic changes that may accompany alterations in local DNA conformation or modifications in drug structure or both. We report a new technique that makes use of specifically deuteriated ^{32}P end-labeled DNAs in combination with gel electrophoresis to detect and quantitate potentially rate-limiting carbon-hydrogen bond cleavages by DNA-cleaving drugs at individual sequence sites. We use BLM as an example.

The activity of BLM in vitro depends on Fe(II) and O_2 or Fe(III) and H_2O_2 (*6*). The initial BLM·Fe(II)·O_2 complex (Fig. 1) undergoes one-electron reduction to ultimately yield "activated BLM," which can initiate DNA damage (*7*). Two types of DNA damage are observed with "activated BLM" (Fig. 2, A and B). Pathway A results in the formation of nucleic acid base propenal and a DNA strand scission that yields 3′-phosphoglycolate and 5′-phosphate termini. Pathway B results in the liberation of nucleic acid base plus an alkali-labile site that cleaves at *p*H 12 with piperidine to afford a 3′-phosphate and a 5′-phosphate terminus. On the basis of the identification of the propenal (*7, 8*), Giloni *et al.* (*8*) inferred that

J. W. Kozarich, L. Worth, Jr., B. L. Frank, D. F. Christner, D. E. Vanderwall, Department of Chemistry and Biochemistry and Center for Agricultural Biotechnology, University of Maryland, College Park, MD 20742.
J. Stubbe, Department of Chemistry, Massachusetts Institute of Technology, Cambridge, MA 02139.

*To whom correspondence should be addressed.

this product was consistent with a 4′-C-H homolytic bond cleavage. The mechanism of release of nucleic acid base and of formation of alkali-labile sites remained obscure, although there was at least one suggestion that this pathway could be explained by a competing 1′-C-H cleavage (*9*).

We proposed a unified mechanism for BLM action (Fig. 2) (*10–14*) based on our studies of BLM reaction with simple DNA polymers [such as poly(dA·dU)] tritiated at specific positions in the deoxyribose ring, which suggested that "activated BLM" effected a 4′-C-H bond cleavage in B-form DNA that was subject to a surprisingly large tritium selection effect (k_H/k_T = 7 to 11). The putative 4′-radical intermediate could be intercepted by O_2 (pathway A) or undergo a hydroxylation (pathway B). Modulation of the O_2 concentration indeed changed the relative ratio of damage by both pathways without a significant effect on the observed selection effect.

Our proposal has not gone without criticism (*15*). Several factors limit the sensitivity of the approach. First, tritium is necessarily used as a tracer isotope, so that extensive DNA damage is required (upwards of 50%) for the accurate quantitation of tritiated products. Second, such large isotope effects can be subject to relatively large errors (*11*) and are global in nature without specific sequence information. Finally, the analysis of the chemistry at minor damage sites is hampered by the lack of sensitivity. We noted, however, that the tritium selection effect predicts a deuterium kinetic isotope effect of ~4 to 5 (*16*)

$$k_H/k_D = 1.44\sqrt{k_H/k_T} = 4 \text{ to } 5 \quad (1)$$

that could be detected at individual sequence sites in a heterogeneous DNA under "one-hit" conditions. We prepared [4′-^{2}H]thymidine 5′-triphosphate (dTTP) with high isotopic content (>95%) and assessed the relative damage at specific sites by electrophoretic separation and quantitation of the set of DNA fragments 5′ end-labeled with ^{32}P. The drug-limiting conditions of a DNA sequence analysis may be viewed as an initial velocity experiment.

The chemical synthesis of [4′-^{2}H]dTTP (>95% ^{2}H) followed published procedures (*17*). The deuteriated nucleotide was incorporated into the (+)-strand of the Eco RI–Bam HI restriction fragment (375 bp) of

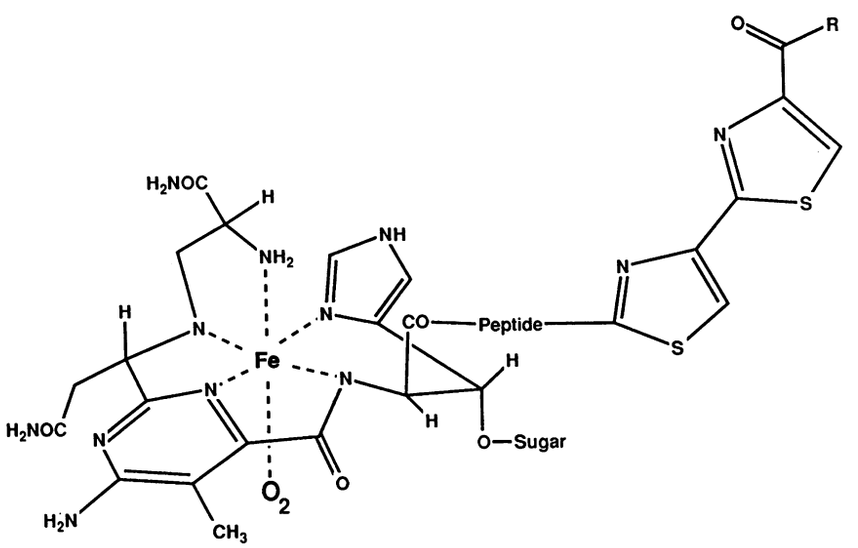

Fig. 1. Proposed structure of the BLM·Fe·O_2 complex.

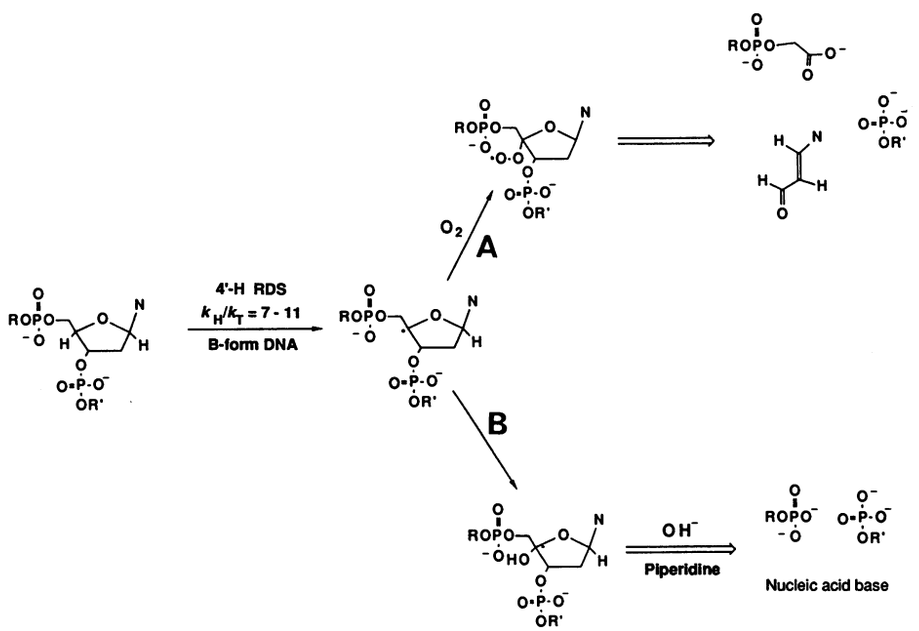

Fig. 2. Proposed unified mechanism for the cleavage of DNA by "activated BLM" (*1, 11–14*).

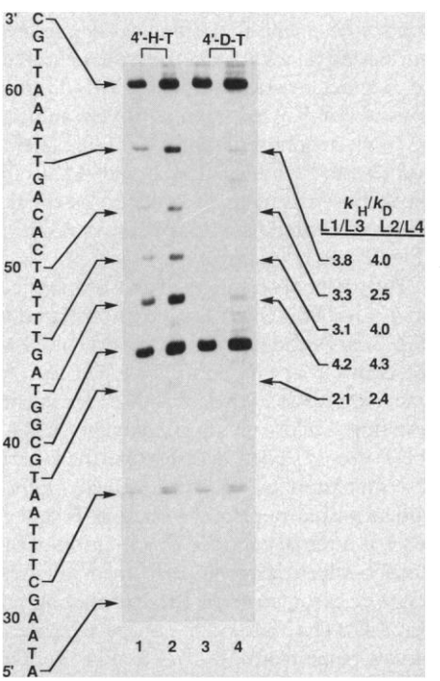

Fig. 3. Autoradiogram of a high-resolution denaturing polyacrylamide gel of the reaction of "activated BLM" and the Eco RI–Bam HI pBR322 fragment containing [4′-^{1}H]T (lanes 1 and 3) or [4′-^{2}H]T (lanes 2 and 4). Each reaction (80 μl) contained 10 m*M* Na_2HPO_4, *p*H 7.6, 10 m*M* β-mercaptoethanol, sonicated salmon sperm DNA (0.2 μg/μl), and ~70,000 cpm of fragment 5′ end-labeled with ^{32}P. The BLM·Fe(II) (1:3) was freshly prepared and added to a final concentration of 3.5 μ*M* (~100 bp per BLM). Reactions were incubated for 10 min at 25°C and terminated by addition of 0.1 m*M* EDTA, 2.5*M* sodium acetate and salmon sperm DNA (0.2 μg/μl) (100 μl final volume). Samples were precipitated with ethanol and subjected to gel electrophoresis (*23*). Samples in lanes 1 and 3 received no alkali treatment (pathway A, Fig. 2). Samples in lanes 2 and 4 were treated with 1*M* piperidine for 15 min at 90°C and repelleted before electrophoresis (pathways A and B, Fig. 2).

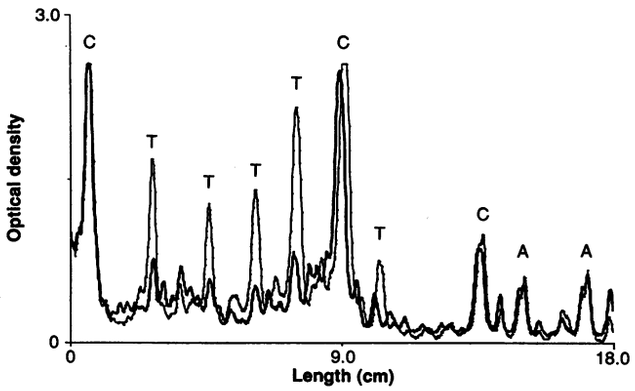

Fig. 4. Densitometry scan of the autoradiogram in Fig. 3. Total strand damage of [4′-^{1}H]T–containing DNA fragment (lane 2, light line) by "activated BLM" is compared to total strand damage of [4′-^{2}H]T–containing DNA fragment (lane 4, heavy line). The ratio of the integrated peak areas is a direct measure of the kinetic isotope effect at that position (L2/L4, Fig. 3). Similar scans were performed on lanes 1 and 3 (L1/L3, Fig. 3). The scans shown are the raw data without normalization.

pBR322 and then the 5′ end of this strand was labeled with ^{32}P (*18–21*). The autoradiogram of the cleavage pattern (*22*) resulting from treatment of this fragment with limiting "activated BLM" is shown in Fig. 3. Identical experiments were performed on a control fragment containing no deuteriated nucleotide (lanes 1 and 2) and the deuteriated fragment (lanes 3 and 4). In addition, control and labeled fragments were subjected to electrophoresis both without (lanes 1 and 3) and with (lanes 2 and 4) alkali-piperidine treatment in order to assess the effects of deuteriation on pathways A and B (Fig. 2) (*23*).

The direct observation of an isotope effect on 4′-C-H bond cleavage is demonstrated in Fig. 3, as is the known preference of BLM for cleavage at GC and GT sequences (*1*). The suppression of [^{32}P]DNA fragments resulting exclusively from damage at [4′-^{2}H]T sites is strong evidence for the kinetic discrimination by "activated BLM." Since undeuteriated nucleotides such as C and A serve as internal controls, quantitation of the isotope effects may be performed by scanning densitometry of the autoradiogram (Fig. 4). The calculated isotope effects exhibit a range from ~2 to 4.5 (Fig. 3). The differences in the magnitude of the effect at different sites is reproducible and suggests that local sequence variability may be important. Dissociation of the "activated BLM" from DNA must also be faster than bond cleavage to permit discrimination between labeled and unlabeled cleavage sites.

The isotope effects on pathways A and B (Fig. 2) are essentially the same for a particular damage site. The isotope effects on pathway A (L1/L3; Fig. 3) were determined by quantitation of neutral strand scission, whereas those on pathways A plus B (L2/L4; Fig. 3) were determined by quantitation of total alkali-induced scission. The effect on pathway B is similar to that on pathway A, which affirms the partitioning of a common intermediate at individual damage sites.

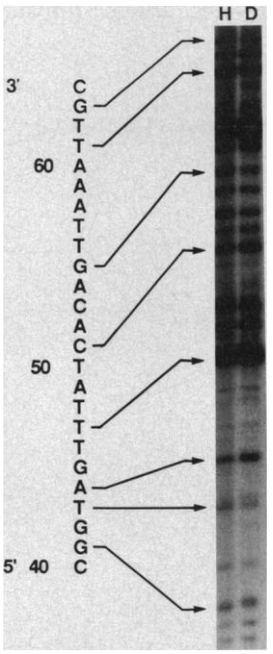

Fig. 5. Autoradiogram of a high-resolution denaturing polyacrylamide gel of the reaction of esperamicin A_1 with the pBR322 fragment containing [4′-^{1}H]T (lane H) or [4′-^{2}H]T (lane D). Each reaction (25 μl) contained 50 m*M* tris-HCl, *p*H 7.5, 0.1 m*M* EDTA, sonicated salmon sperm DNA (0.2 μg/μl), and ~164,000 cpm of a fragment 5′ end-labeled with ^{32}P. Esperamicin A_1 (50 μ*M*; 1 μl) was added and the solution was incubated at room temperature for 20 min. Dithiothreitol (25 m*M*; 1 μl) was then added and the reaction was incubated at 37° for 10 min. The reaction was terminated by addition of 0.1 m*M* EDTA, 2.5*M* sodium acetate and salmon sperm DNA (0.2 μg/μl) (50 μl final volume). Samples were precipitated with ethanol and subjected to gel electrophoresis (*23*).

Moreover, preliminary experiments varying the O_2 concentration to alter the partition ratio corroborate this proposal.

The isotope effects are clearly dependent on the nature of the DNA cleaver. Experiments performed with esperamicin A_1 (*4*) revealed, in addition to a substantially different sequence specificity, no significant isotope effect on 4′-C-H bond cleavage (Fig. 5). While this result does not exclude this cleavage as a mode of action of esperamicin, it does rule out this step as a rate-determinant. The results, nevertheless, constitute a convincing control.

REFERENCES AND NOTES

1. J. Stubbe and J. W. Kozarich, *Chem. Rev.* **87**, 1107 (1987).
2. I. H. Goldberg, *Free Radical Biol. & Med.* **3**, 41 (1987).
3. N. Zein, A. M. Sinha, W. J. McGahren, G. A. Ellestad, *Science* **240**, 1198 (1988); N. Zein, M. Poncin, R. Nilakantan, G. A. Ellestad, *ibid.* **244**, 697 (1989).
4. B. H. Long *et al.*, *Proc. Natl. Acad. Sci. U.S.A.* **86**, 2 (1989).
5. P. B. Dervan, *Science* **232**, 464 (1986); D. S. Sigman, *Acc. Chem. Res.* **19**, 180 (1986); J. K. Barton, *Science* **233**, 727 (1986); K. C. Nicolaou, Y. Ogawa, G. Zuccarello, H. Kataoka, *J. Am. Chem. Soc.* **110**, 4866 (1988).
6. E. A. Sausville, J. Peisach, S. B. Horwitz, *Biochem. Biophys. Res. Commun.* **73**, 814 (1976); E. A. Sausville, R. W. Stein, J. Peisach, S. B. Horwitz, *Biochemistry* **17**, 2746 (1978).
7. R. M. Burger, J. Peisach, S. B. Horwitz, *J. Biol. Chem.* **256**, 11636 (1981).
8. L. Giloni, M. Takeshita, F. Johnson, C. Iden, A. Grollman, *ibid.*, p. 8608.
9. S. M. Hecht, in *Bleomycin: Chemical, Biochemical, and Biological Aspects*, S. M. Hecht, Ed. (Springer-Verlag, New York, 1979), pp. 1–23.
10. J. C. Wu, J. W. Kozarich, J. Stubbe, *J. Biol. Chem.* **258**, 4694 (1983).
11. ———, *Biochemistry* **24**, 7562 (1985).
12. J. C. Wu, J. Stubbe, J. W. Kozarich, *ibid.*, p. 7569.
13. S. Ajmera *et al.*, *ibid.* **25**, 6586 (1986).
14. L. E. Rabow, J. Stubbe, J. W. Kozarich, J. A. Gerlt, *J. Am. Chem. Soc.* **108**, 7130 (1986).
15. M. R. Ciriolo, J. Peisach, R. S. Magliozzo, *J. Biol. Chem.* **264**, 1443 (1989).
16. C. G. Swain, E. C. Stivers, J. F. Reuwer, Jr., L. J. Schaad, *J. Am. Chem. Soc.* **80**, 5885 (1958).
17. S. Ajmera and J. W. Kozarich, *J. Labelled Compd. & Radiopharm.* **23**, 963 (1986).
18. The Eco RI–Bam HI restriction fragment (375 bp) from pBR322 was cloned into M13mp19, and the single-stranded DNA was isolated from infected *Escherichia coli*, JM101 (*19, 20*). Synthesis of the complementary strand was accomplished by annealing kinase-treated primer to the single-stranded template and by performing the polymerization with Sequenase (U.S. Biochemicals) and with dGTP, dATP, dCTP, and either dTTP or [4′-^{2}H]dTTP. The polymerization and terminal ligation was monitored by comparison to replicative form on agarose gels. Samples were purified on Sephadex G-50 (*21*). The prepared replicative form containing either [4′-^{1}H]- or [4′-^{2}H]T was treated with Eco RI (1 hour, 37°) and 5′end-labeled by standard procedures (*21*). The desired 375-bp fragment was produced by Bam HI digestion, resolved by electrophoresis on a 5% acrylamide gel and purified on an NACS Prepac (BRL) column.
19. F. Sanger, S. Miklen, A. R. Coulson, *Proc. Natl. Acad. Sci. U.S.A.* **74**, 5463 (1977).
20. J. Messing, *Methods Enzymol.* **101**, 20 (1983).
21. T. Maniatis, E. F. Fritsch, J. Sambrook, *Molecular Cloning: A Laboratory Manual* (Cold Spring Harbor Laboratory, Cold Spring Harbor, NY, 1982).
22. A. M. Maxam and W. Gilbert, *Methods Enzymol.* **65**, 499 (1980).
23. Since pathway A leads to 3′-phosphoglycolate termini and pathway B to 3′-phosphate termini, the corresponding oligomeric fragments are separable on high-resolution gels under certain conditions, which is especially apparent in Fig. 3 for the smallest fragments (see A and C damage sites at bottom of autoradiogram). Thus lanes 1 and 2 yield a predominant band corresponding to the 3′-phosphoglycolate ends generated under neutral conditions, and

lanes 2 and 4 reveal an additional band of slower mobility corresponding to the 3′-phosphate ends produced by the alkali-piperidine treatment. The resolution is lost as fragment size increases, but this has no effect on the subsequent interpretation of the experiment.

24. We thank G. Freeman and T. D. Tullius for helpful advice and for use of the scanning densitometer. A gift of esperamicin A_1 was provided by B. Krishnan and T. W. Doyle. Supported by an American Cancer Society Faculty Research Award (J.W.K.), NIH Research Career Development Award (J.S.), and NIH grant GM 34454.

23 May 1989; accepted 14 August 1989

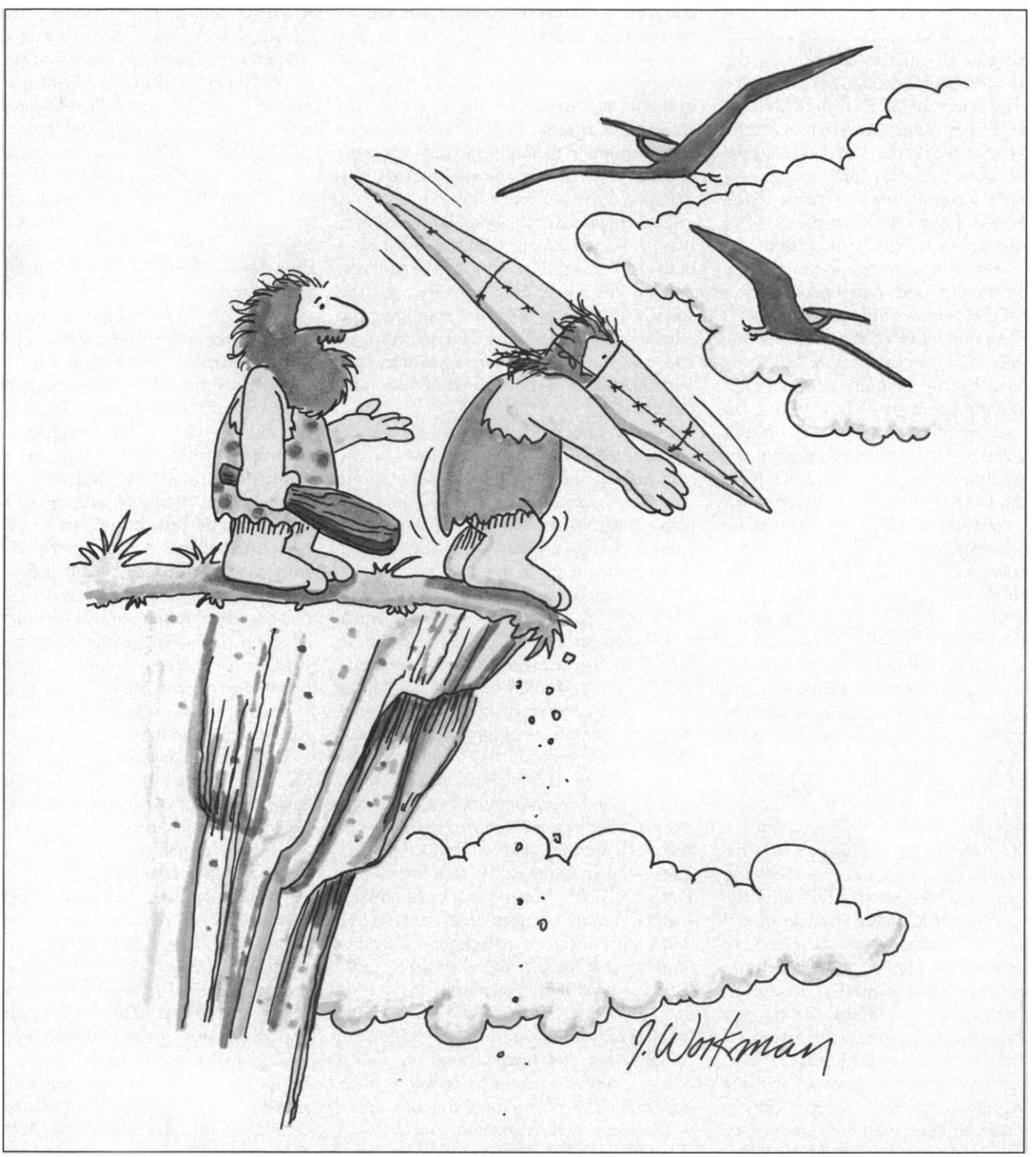

"Are you sure about this, Stan? It seems odd that a pointy head and long beak is what makes them fly."